POLYMER REACTION ENGINEERING, 10(1&2), 59–82 (2002)

EMULSION COPOLYMERIZATION OF ACRYLONITRILE AND BUTADIENE. SEMIBATCH STRATEGIES FOR CONTROLLING MOLECULAR STRUCTURE ON THE BASIS OF CALORIMETRIC MEASUREMENTS

J. R. Vega, L. M. Gugliotta, and G. R. Meira*

INTEC (Universidad Nacional del Litoral and CONICET), Güemes 3450, (3000) Santa Fe, Argentina

ABSTRACT

A semibatch emulsion copolymerization of acrylonitrile and butadiene is theoretically investigated, with the aim of controlling the molecular structure of the produced NBR. An open-loop estimator based on calorimetric measurements is proposed for monitoring the chemical composition, the average molecular weights, and the average degree of branching. With little effect on the other quality variables, the intermediate addition of acrylonitrile allows to produce a polymer with a constant chemical composition. Similarly, the intermediate addition of the chain transfer agent produces a polymer with either a fixed $\overline{M}_w$ or with a

*Corresponding author.

prespecified linear variation of the average branching. The required feed profiles are obtained from a numerical inversion of a discrete process model. By increasing the initiator loads, the semibatch strategies also allow to increase the final conversion between 3% and 6%, without altering the reaction time nor deteriorating the polymer quality with respect to the batch. The numerical procedures were tested by inputing (relatively noisy) heat measurements from an industrial batch reactor.

INTRODUCTION

Nitrile rubber or NBR is industrially produced by polymerizing acrylonitrile (A) and butadiene (B) in the "cold" emulsion process.[1] The reactor can be either batch, semibatch, or a train of continuous stirred-tanks.

The molecular characteristics of NBR are determined by the copolymer composition, the molecular weights, and the degree of branching. The most common NBR type (the BJLT grade), contains a mass fraction of bound A of about 35%. This value is close to the azeotropic composition of 38%;[2] therefore, the BJLT grade exhibits only a slight compositional drift when produced in a batch reactor. The other commercial grades contain lower amounts of bound A, and normally require a composition control via semibatch addition of A.[3] The molecular weights are limited by including a chain transfer agent (CTA) or "modifier" in the reaction recipe. Finally, the average degree of branching is maintained below certain limits by limiting the final conversion to around 75%.

Industrial NBR processes normally involve on-line measurements of the reaction temperature; and off-line measurements of conversion, copolymer composition, and Mooney viscosity. The varying amounts of oxygen and other impurities in the reaction system determine that relatively large batch-to-batch variations are observed in the conversion and in the quality variables.

Recent publications on the mathematical modeling of the NBR emulsion process were produced by Vega et al.,[3] Dubé et al.,[4] and Rodríguez et al.[5] This last publication estimates the MWD of each generated branched topology; where each topology is characterized by the number of branching points per molecule.

The batch-to-batch variations in the impurity contents determine that open-loop models are unable to predict the real evolution of the main process variables. Such predictions can be considerably improved if the conversion is on-line measured or estimated. For example, Leiza et al.[6] have used on-line gas chromatography (GC) to measure conversion and to control copolymer composition in a semibatch copolymerization of ethyl acrylate and methyl

methacrylate. Canegallo et al.[7] employed on-line densitometry to monitor conversion and to control copolymer composition in several co- and terpolymerizations. Van den Brink et al.[8] utilized on-line Raman spectroscopy to monitor conversion and copolymer composition in the batch copolymerization of n-butyl acrylate and vinyl neononanoate; and to control copolymer composition in a semibatch operation. By carrying out the polymerizations in a commercial calorimeter, several variables have been estimated and controlled. For example, Sáenz de Buruaga et al.[9–12] controlled copolymer composition in several co- and terpolymerizations. Via a simultaneous feed of CTA and/or of comonomers, Vicente et al.[13,14] produced linear homopolymers with prespecified MWDs, and linear copolymers with controlled MWDs and copolymer compositions.

Kozub and MacGregor[15] simulated a semi-batch emulsion copolymerization of styrene and butadiene with the aim of controlling conversion, copolymer composition, weight-average molecular weight, and degree of branching. To this effect, a model-based open-loop controller was developed, and the following on-line measurements were assumed: GC, light scattering, and CTA titration. The control scheme also included an external feedback loop for reducing the errors introduced by model mismatch and/or by uncertainties in the initial loads. As far as the authors are aware, no publications have appeared on the estimation and control of the degree of branching on the basis of calorimetric measurements.

In Gugliotta et al.,[16] a simplified process model was used in combination with energy measurements for monitoring conversion, copolymer composition, and average molecular weights. To this effect, three open-loop estimators were developed, and a good agreement between on-line estimates and off-line measurements was obtained.

The present work is a continuation of the mentioned publication by Gugliotta et al.[16] First, an open-loop estimator is presented that monitors the average number of branching points per molecule. Then, three semibatch strategies are proposed for controlling copolymer composition, molecular weights, or degree of branching. Finally, the problem of increasing the monomer conversion without deteriorating the polymer quality is investigated.

THE BATCH POLYMERIZATION AND THE ON-LINE ESTIMATOR

Reconsider the batch emulsion copolymerization of A and B for producing a grade BJLT NBR, that has been previously reported in Gugliotta et al.[16] The reaction was carried out in a 21 000 dm^3 industrial stirred-tank reactor (Pecom Energía S.A., Argentina); and the recipe was as follows: A: 2048 Kg; B: 4475 Kg; emulsifier: 230 Kg; initiator (di-isobutyl hydroperoxide): 0.32 Kg; CTA (*tert*-

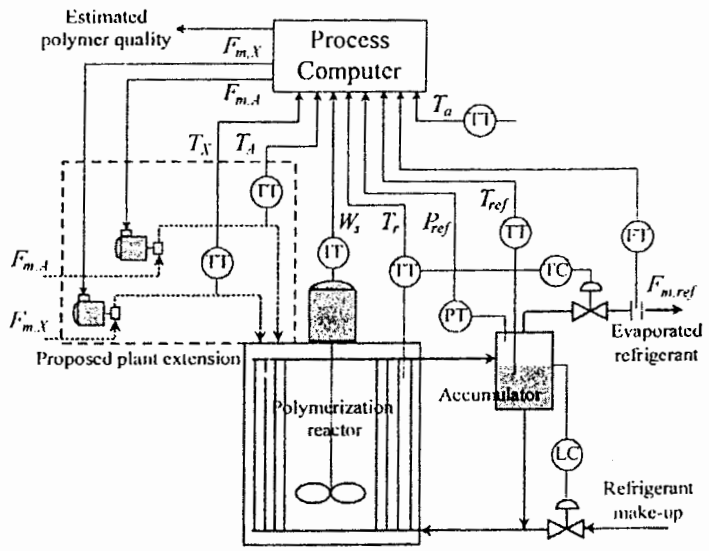

Figure 1. Industrial batch reactor and proposed extension to allow the semi-batch operations.

dodecyl mercaptan): 26.7 Kg; and water: 11100 Kg. The batch reactor is schematically represented in Figure 1, and it did not include the elements indicated in "proposed plant extension." A propane-propylene refrigerant circulates through an internal set of vertical tubes laid out to operate as reactor baffles. The reaction heat was mainly removed by the evaporated refrigerant. The reaction temperature was held at approximately 10°C by means of an external control loop. A second control loop maintained a constant level of refrigerant in the accumulator.

Except for the initiator, all other reagents were first emulsified and cooled to the reaction temperature. The polymerization started when the initiator was loaded. The following variables were measured on-line every $\Delta t = 2$ min: the reaction temperature, T_r (Figure 2a); the ambient and refrigerant temperatures, T_a and T_{ref} (Figure 2a); the stirring power, W_s; the evaporated refrigerant mass flow, $F_{m,ref}$ (Figure 2b); and the refrigerant pressure, P_{ref}. The estimated reaction heat, Q_r, is presented in Figure 2b. As expected, an almost direct proportionality between Q_r and $F_{m,ref}$ is observed.[16]

Latex samples were withdrawn along the copolymerization, and the following analyses were carried out (see Figure 2c–e): a) the gravimetric conversion, x_g, following ASTM B 1417-80; b) the average mass fraction of A in the copolymer, $\overline{p}_A$, through the Kjeldahl method;[17] and c) the average molecular

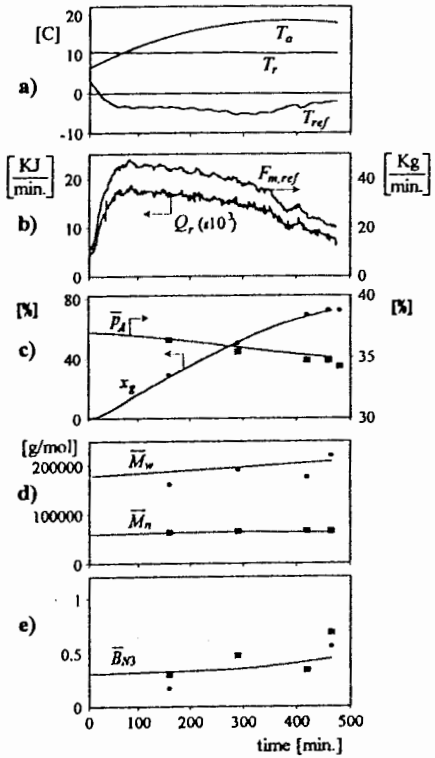

Figure 2. Batch experiment: main variables. (a) Measured temperatures, T_a, T_r, and T_{ref}; (b) measured refrigerant mass flow, $F_{m,ref}$, and estimated reaction heat rate, Q_r; (c) gravimetric conversion, x_g, and average mass fraction of A in the copolymer, $\overline{p}_A$; (d) average molecular weights, $\overline{M}_n$ and $\overline{M}_w$; (e) average number of trifunctional branches per copolymer molecule, $\overline{B}_{N3}$. (On-line measurements and estimates are shown in continuous trace. Off-line measurements are shown in symbols. In (e), the dots are SEC-viscometry measurements, whereas the squares were indirectly estimated from polydispersity measurements (see bottom of Table 1).

weights and the (number–average) number of branches per molecule, $\overline{B}_{N3}$, through a Waters ALC220 size exclusion chromatograph fitted with a Viscotek 200 on-line viscometer.

To determine $\overline{B}_{N3}$ by SEC-viscometry, the following was required: i) a universal calibration; ii) the Mark–Houwink parameters of a linear NBR in a range of molecular weights similar to that of the measured copolymer; and iii) the ε exponent in $g^{\varepsilon}(M) = g'(M)$, where $g(M)$ is the branching function based on

Table 1. Batch Polymerization: Final Polymer Characteristics

	x_g (%)	$\bar{p}_A$ (%)	$\overline{M}_n$ (g/mol)	$\overline{M}_w$ (g/mol)	$\overline{B}_{N3}$ (br./molec.)
Measurement	72.1	34.2	65200[a]	220000[a]	0.56[a]; 0.687[b]
Model prediction	71.7	35.0	62700	208000	0.45

[a] By SEC-viscometry.
[b] Indirectly calculated from: $\overline{B}_{N3} = 0.5\ (\overline{M}_w/\overline{M}_n - 2)$.

molecular sizes and $g'(M)$ is the branching function based on intrinsic viscosities. The Mark–Houwink parameters were determined from intrinsic viscosity measurements of (almost linear) NBR samples produced at a very low conversion. The ε exponent was adjusted to 0.7, after comparing the SEC estimations of $g'(M)$ with theoretical predictions of $g(M)$.[18,19] Additionally, the average degree of branching was indirectly estimated from the molecular weight polydispersity using the empirical correlation shown at the bottom of Table 1.[20,21]

The initial comonomer ratio is somewhat below the azeotropic composition, and, for this reason, a decreasing mass fraction of A in the copolymer is observed ($\bar{p}_A$ in Figure 2c). The variation of $\overline{M}_n$ is very moderate (Figure 2d), and this is a consequence of an almost constant ratio between the rate of propagation and the rate of chain transfer to the CTA. The branching reactions increase with conversion; and this explains the increasing profiles of $\overline{B}_{N3}$ and $\overline{M}_w$ (Figure 2d,e). The final polymer characteristics are given in Table 1.

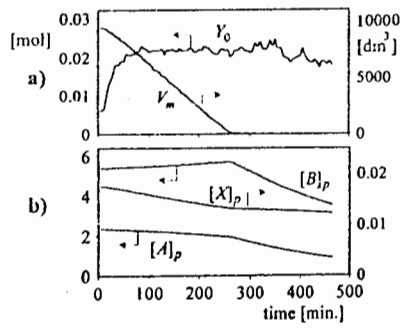

Figure 3. Batch experiment: some estimated intermediate variables. (a) Total free-radical moles in the polymer phase, Y_0, and monomer phase volume, V_m; and (b) monomers and CTA concentrations in the polymer phase, $[A]_p$, $[B]_p$, and $[X]_p$.

All estimates were based on the evolution of the reaction heat Q_r; that in turn was evaluated through Eq. A.8. The estimates for x_g, $\bar{p}_A$, $\overline{M}_n$, and $\overline{M}_w$ of Figure 2c,d were directly taken from Ref. 16. For $\overline{B}_{N3}$, the corresponding on-line estimator is derived in the APPENDIX (Eq. A.9.a), and the estimates are presented in Figure 2e). The final polymer predictions are given in Table 1.

Figure 3 presents the predicted evolution of some important intermediate variables such as the total moles of free radicals in the polymer phase, Y_0 (obtained from Eq. A.10); the monomer phase volume, V_m; and the concentration of the comonomers and the CTA in the polymer particles, $[A]_p$, $[B]_p$, and $[X]_p$. Note the following: a) the oscillations in $Y_0(t)$ are a result of the oscillations in $Q_r(t)$ (Figure 2b); b) the interval II of the emulsion polymerization finishes at $t \cong 270$ min., when the monomer phase volume disappears; c) the concentration of comonomers in the polymer phase are relatively constant while the monomer phase is still present, and thereafter they decrease; and d) the concentration of CTA in the polymer phase decreases monotonically along the reaction.

THE CONTROL ALGORITHM

Consider now the semibatch system of Figure 1, which includes the proposed hardware extension. The mass feed of A, $F_{m,A}$, is used to control the copolymer composition, while the mass feed of X, $F_{m,X}$, is used to control either $\overline{M}_n$, $\overline{M}_w$, or $\overline{B}_{N3}$. Note that the comonomer feeds were not considered for controlling $\overline{B}_{N3}$. The temperature of the applied feed (either T_A or T_X), is on-line measured.

The equations for the model-based control are presented in the Appendix. The copolymer composition control aims at producing a fixed and prespecified mass fraction of A, $\bar{p}_A^d$. The initial charge of A, N_A^0, and the required mass flow of A, $F_{m,A}(t)$, are obtained from Eqs. A.11–A.14. To solve these equations, the following intermediate variables must be either measured or estimated: $Y_0(t)$, $[B]_p(t)$, and the unreacted moles of A, $N_A(t)$.

The control of $\overline{M}_w$ aims at producing a polymer with $\overline{M}_w(t) = \overline{M}_w^d$. The necessary CTA profile, $F_{m,X}$, is obtained through Eq. A.16; and the required CTA concentration in the polymer particles, $[X]_p^d$, is calculated from Eq. A.17. To solve Eqs. A.16 and A.17, the following intermediate variables must be on-line estimated: $Y_0(t)$; the total monomer concentration, $[M]_p(t)$ $(= [A]_p(t) + [B]_p(t))$; the unreacted moles of X, $N_X(t)$; the polymer phase volume, $V_p(t)$; and the MWD moments, $Q_1(t)$ and $Q_2(t)$.

In the control of $\overline{B}_{N3}$, a fixed value of this variable cannot be specified without seriously affecting the other quality variables. Instead, a trajectory with

an increasing $\overline{B}_{N3}^{d}$ has to be chosen. The necessary CTA profile is again obtained through Eq. A.16, but in this case the CTA concentration in the polymer particles is calculated from Eq. A.19. The algorithm requires the input of the following intermediate variables: $Y_0(t)$, $[M]_p(t)$, $N_X(t)$, $V_p(t)$, and $Q_1(t)$.

The proposed estimation and control algorithms are based on finite-difference equations. These equations are very simple to implement on a process computer, but may lead to deviations in the presence of a measurement noise. This problem was particularly observed in the control of $\overline{B}_{N3}$. As an alternative to the model-based control, an algorithm based on a virtual P+D controller[22] was also proposed (Eqs. A.20a,b). The P+D controller requires an estimate of $\overline{B}_{N3}$; that in this case was calculated through Eq. A.9.a.

SIMULATION RESULTS

In what follows, the proposed estimation and control strategies are numerically evaluated. The industrial process was simulated using the polymerization model of Vega et al.[3] The model parameters were taken from Rodríguez et al.,[5] and are reproduced in Table 2.

In a real control situation, $Y_0(t)$ is estimated from the heat rate measurement $Q_r(t)$. In the simulated examples that follow, $Q_r(t)$ is obtained from the batch $Y_0(t)$ profile of Figure 3a. The reason for this is that $Y_0(t)$ mainly

Table 2. Model Parameters (at 10 °C)

Parameter[a]	Value	Reference
k_{pAA}	3.98×10^5 dm^3/mol min.	[23]
k_{pBB}	5.30×10^2 dm^3/mol min.	[3]
$k_{fAA}=k_{fBA}$	2.00 dm^3/mol min.	[23]
$k_{fAB}=k_{fBB}$	0.01 dm^3/mol min.	[24]
$k_{fpAA}=k_{fpBA}$	1.10 dm^3/mol min.	[23]
$k_{fpAB}=k_{fpBB}$	0.055 dm^3/mol min.	[24]
k_{fAX}	1.28×10^5 dm^3/mol min.	[23]
k_{fBX}	2.41×10^2 dm^3/mol min.	[3]
$k_{pA}^{*}=k_{pB}^{*}$	9.56×10^{-3} dm^3/mol min.	[24]
$r_A=k_{pAA}/k_{pAB}$	0 03	[16]
$r_B=k_{pBB}/k_{pBA}$	0.30	[16]
ΔH_A	−76.3 KJ/mol	[23]
ΔH_B	−73.0 KJ/mol	[23]

[a]see Nomenclature.

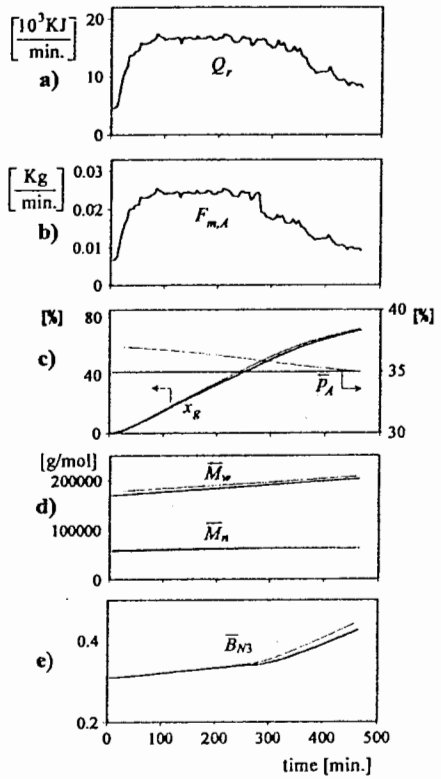

Figure 4. Control of copolymer composition (simulation results). (a) "Measured" reaction heat rate, Q_r; (b) required mass flow of A, $F_{m,A}$; (c) gravimetric conversion, x_g, and average mass fraction of A in the copolymer, $\overline{p}_A$; (d) average molecular weights, $\overline{M}_n$ and $\overline{M}_w$; and (e) average number of trifunctional branches per molecule, $\overline{B}_{N3}$. (For comparison, the batch predictions are reproduced in continuous thin trace.)

depends on the concentrations of emulsifier and initiator, and it is, therefore, quite independent of the semibatch policies. The injection of (the relatively noisy) $Y_0(t)$ of Figure 3a into the control algorithms allows the testing of the proposed procedures in a realistic fashion. In summary, for the computer simulation, the "measurement" $Q_r(t)$ was calculated from the $Y_0(t)$ of Figure 3a, as follows:

$$Q_r = R_{pA}(-\Delta H_A) + R_{pB}(-\Delta H_B) \tag{1}$$

with

$$R_{pA} = \frac{k_{pAA}k_{pBB}\left(r_A[A]_p^2 + [A]_p[B]_p\right)Y_0}{k_{pBB}r_A[A]_p + k_{pAA}r_B[B]_p} \tag{2.a}$$

$$R_{pB} = \frac{k_{pAA}k_{pBB}\left(r_B[B]_p^2 + [A]_p[B]_p\right)Y_0}{k_{pBB}r_A[A]_p + k_{pAA}r_B[B]_p} \tag{2.b}$$

where ΔH_A, ΔH_B are the molar polymerization enthalpies of A and B; R_{pA}, R_{pB} are the consumption rates of A and B; k_{pAA}, k_{pBB} are the homopropagation rate constants for A, B; and r_A, r_B are the reactivity ratios of A, B.

Control of Copolymer Composition

The aim here is to produce a copolymer with the following flat evolution of the chemical composition: $\bar{p}_A(t) = \bar{p}_A^d = 0.35$. Figure 4a presents the "measurement" $Q_r(t)$ obtained from Eqs. 1 and 2.a,b. The initial load of A was, in this case, $N_A^0 = 1681$ Kg; while all the other initial loads coincided with the batch operation. The required feed profile of A is presented in Figure 4b. Note that while a monomer phase is present (*i.e.*, until $t \cong 270$ min.), the required feed is almost proportional to $Q_r(t)$. This is to be expected from Eq. A.15 under pseudo-bulk conditions for the partitioning of the comonomers.

Figure 4c–e represent the simulated evolution of the main variables. As expected, a uniform-composition copolymer is produced. For comparison, the batch evolutions are also included in Figure 4c–e. The final polydispersity and the final degree of branching are lower than in the batch, with negligible effects on $x_g(t)$ and $\overline{M}_n(t)$.

Control of the Weight-Average Molecular Weight

The aim here is to produce a polymer with $\overline{M}_w(t) = \overline{M}_w^d = 200000$ g/mol. Since the addition of CTA has an almost negligible effect on the polymerization rate, then one can directly adopt the $Y_0(t)$ and $Q_r(t)$ profiles of the batch operation. Except for the initial charge of CTA ($N_X^0 = 22.8$ Kg), all other initial conditions coincided with the batch. The required CTA profile is shown in Figure 5a. Figure 5b indicates that it is indeed possible to produce the required flat profile of $\overline{M}_w(t)$. The evolutions of x_g, $\bar{p}_A$, and V_m almost coincide with the

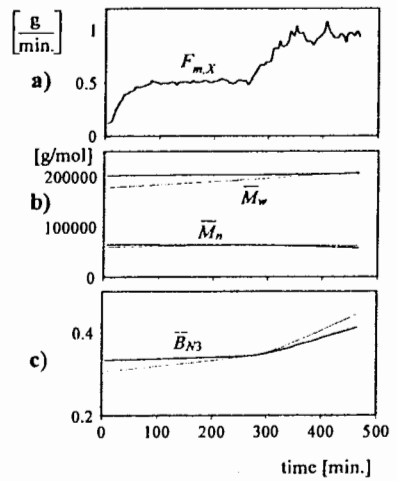

Figure 5. Control of $\overline{M}_w$ (simulation results). (**a**) Required mass flow of chain transfer agent, $F_{m,X}$; (**b**) average molecular weights, $\overline{M}_n$ and $\overline{M}_w$; and (**c**) average number of trifunctional branches per molecule, $\overline{B}_{N3}$. (For comparison, the batch predictions are also reproduced in continuous thin trace.)

corresponding batch evolutions, and for this reason they are not reproduced here. The average molecular weights and the average degree of branching are represented in Figure 5b,c. The final $\overline{B}_{N3}$ is lower than in the batch, but the polydispersity is slightly higher.

Control of Branching

The aim here was to reproduce the linear variation for $\overline{B}_{N3}(t)$, as represented by $\overline{B}_{N3}^d(t)$ in Figure 6c. Such profile was selected by extrapolation of the almost linear profile of $\overline{B}_{N3}(t)$ observed during intervals I and II of the batch polymerization. All initial conditions coincide with the batch; as before, the batch evolutions for $Y_0(t)$ and $Q_r(t)$ are here readopted. In this case, the model-based control of Eqs. A.16 and A.19 failed to produce the required evolution of $\overline{B}_{N3}$. The feed profile that meets the control objective was calculated with the virtual P+D controller of Eqs. A.20.a,b. The CTA profiles obtained via the two calculation methods are shown in Figure 6a. Note that an increased CTA feed is necessary after disappearance of the monomer droplets at $t \cong 270$ min. Also, the final $\overline{B}_{N3}$ and average molecular weights are all lower than in the batch (Figure 6b,c).

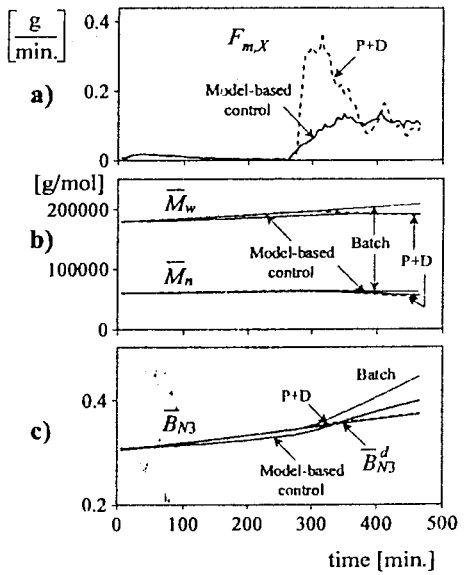

Figure 6. Control of the degree of branching (simulation results). Outputs from the model-based controller are indicated in thick trace, while outputs from the P + D controller are indicated in dashed trace. (a) Required mass flow of CTA, $F_{m,X}$; (b) average molecular weights, $\overline{M}_n$ and $\overline{M}_w$; and (c) average number of trifunctional branches per molecule, $\overline{B}_{N3}$. (For comparison, batch predictions are also reproduced in continuous thin trace.)

Increasing the Final Conversion

In Figures 4–6, the final conversions almost coincide with the final batch conversion. Reconsider now the previously described strategies, but with the added aim of increasing the final conversion without increasing the reaction time nor deteriorating the polymer quality. To this effect, higher initiator loads m_I are necessary; therefore, the $Y_0(t)$ profile is expected to be higher than in the batch (Figure 3a). The new $Y_0(t)$ profile was estimated from: $Y_0(t) = Y_{0,\text{batch}}(t)\,[m_I/m_{I,\text{batch}}]^{0.4}$. This expression is the result of assuming the Harkins' mechanism of nucleation and a constant $\bar{n}$ in the emulsion process. The resulting initiator loads are given in Table 3.

The control objectives were in all cases satisfied; Table 3 exhibits the final rubber properties. The following can be noted: a) when controlling the chemical composition, the final conversion can be increased by about 3% with respect to the batch, with a reduced polydispersity; b) when controlling $\overline{M}_w$, the conversion can be increased by about 6% with a negligible effect on $\overline{B}_{N3}$, but with a somewhat reduced $\overline{M}_n$ and an increased polydispersity; and c) when controlling $\overline{B}_{N3}$, the conversion can be also increased by about 6%, but with a slight drop in the average molecular weights.

Table 3. Final Properties with Increased Final Conversions

	Batch Reaction	Control Objective in Semibatch Policy		
		$\overline{p}^d_A = 0.35$	$\overline{M}^d_w = 200000$	$\overline{B}^d_{N3}(t)$[a]
m_I (Kg)	0.320	0.387	0.378	0.378
x_g (%)	71.7	74.0	75.8	75.8
$\overline{p}_A$ (%)	35.0	35.0	34.7	34.7
$\overline{M}_n$ (g/mol)	62600	62300	55600	52000
$\overline{M}_w$ (g/mol)	208400	205800	206900	188900
$\overline{M}_w/\overline{M}_n$	3.33	3.30	3.72	3.63
$\overline{B}_{N3}$	0.45	0.45	0.44	0.41

[a] $\overline{B}^d_{N3}(t) = 0.304 + 1.5\times10^{-4}t$.

CONCLUSIONS

Conversion can be accurately estimated from calorimetric measurements; and this allows to apply open-loop observers for controlling the polymer quality. However, open-loop estimators cannot compensate for errors in the initial loads and/or in the model parameters. In this case, additional on-line measurements would be required.

The simulation results show that it is possible to independently control the copolymer composition, the weight-average molecular weight, or the average degree of branching. By controlling the composition, the final conversion can be increased by approximately 3% with respect to the batch, without deteriorating the other quality variables. By controlling $\overline{M}_w$ or $\overline{B}_{N3}$, the final conversion can be increased by about 6% with respect to the batch, but at the cost of a slight increase in the molecular weight polydispersity.

The proposed control policies were not experimentally validated. The predicted differences in $\overline{M}_w$ between the semibatch and the batch runs were small because the desired $\overline{M}_w$ was chosen identical to the corresponding final batch value; therefore, their differences are perhaps within experimental errors (e.g., when determined by size exclusion chromatography). For the experimental validation of the $\overline{M}_w$ control strategy, an $\overline{M}^d_w$ significantly different than that of the batch would be required.

The mechanism that determines the copolymer composition is basically decoupled from the mechanism that determines the molecular weights or the

degrees of branching. For this reason, a simultaneous control of $\bar{p}_A$ with either $\bar{M}_w$ or $\bar{B}_{N3}$ seems a priori perfectly feasible.

NOMENCLATURE

A, B	acrylonitrile, butadiene
$\bar{B}_{N3}$, $\bar{B}_{N4}$	number average number of tri- and tetrafunctional branches per molecule (dimensionless)
C_k	(k_p^*/k_p) ratio between the pseudo-rate constant of propagation with the polymer and the pseudo-rate constant of propagation with the monomers (dimensionless)
C_m	(k_{fm}/k_p) ratio between the pseudo-rate constant of transfer to the monomer and the pseudo-rate constant of propagation (dimensionless)
C_p	(k_{fp}/k_p) ratio between the pseudo-rate constant of transfer to the polymer and the pseudo-rate constant of propagation (dimensionless)
c_p^i	specific heat of reagent i (i = A, B, X, copolymer, and water) (KJ/Kg C)
C_p^{if}	heat capacity of the internal fittings (KJ/C)
C_p^i	heat capacity of reagent i (i = A, B, X, copolymer, and water) (KJ/C)
C_X	(k_{fX}/k_p) ratio between the pseudo-rate constant of transfer to the modifier and the pseudo-rate constant of propagation (dimensionless)
$F_{m,i}$	mass flow of reagent i (i = A, X) (Kg/min.)
$F_{m,ref}$	refrigerant mass flow (Kg/min.)
g, g'	branching parameters defined by the ratio of radii of gyration and by the ratio of intrinsic viscosities, respectively (dimensionless)
$[i]_p$	concentration of species i (i = A, B, X) in the polymer phase (mol/dm^3)
K	constant defined by Eq. A.13 (dimensionless)
k	$(t/\Delta t)$ = zdiscrete time (dimensionless)
k_{fAX}, k_{fBX}	transfer to the CTA rate constants for radicals terminated in A and B units (dm^3/mol min.)
k_{fij}	rate constant of transfer between a radical i and a comonomer j (i, j = A,B) (dm^3/mol min.)
k_{fM}	$\{\varphi_A(k_{fAA}[A]_p + k_{fAB}[B]_p)+(1-\varphi_A)(k_{fBA}[A]_p + k_{fBB}[B]_p)\}/\{[A]_p+[B]_p\}$ pseudo-rate constant of transfer to the monomer (dm^3/mol min.)
k_{fp}	$\{\lfloor\varphi_A k_{fpAB} + (1-\varphi_A)k_{fpBB}\rfloor(1-y_A) + \lfloor\varphi_A k_{fpAA} + (1-\varphi_A)k_{fpBA}\rfloor y_A\}$ pseudo-rate constant of transfer to the polymer (dm^3/mol min.)

k_{fpij}	rate constant of transfer between a radical i and a polymerized comonomer j (i, j = A,B) (dm^3/mol min.)
k_{fX}	$[\varphi_A k_{fAX} + (1-\varphi_A)k_{fBX}]$ pseudo-rate constant of transfer to the CTA (dm^3/mol min.)
K_{imp}	partition coefficient of reagent i (i = A, B) between the monomer phase and the polymer phase (dimensionless)
K_{imw}	partition coefficient of reagent i (i = A, B) between the monomer phase and the aqueous phase (dimensionless)
K_{iwp}	partition coefficient of reagent i (i = A, B) between the aqueous phase and the polymer phase (dimensionless)
k_p	$\{\varphi_A(k_{pAA}[A]_p + k_{pAB}[B]_p) + (1-\varphi_A)(k_{pBA}[A]_p + k_{pBB}[B]_p)\}/\{[A]_p + [B]_p\}$ pseudo-rate constant of propagation in the polymer phase (dm^3/mol min.)
k_p^*	$\{\lfloor\varphi_A k_{pA}^* + (1-\varphi_A)k_{pB}^*\rfloor(1-y_A)\}$ pseudo-rate constant of reaction with internal double-bonds (dm^3/mol min.)
k_{pA}^*, k_{pB}^*	rate constant of propagation between A- or B-terminated radicals with internal double bonds (dm^3/mol min.)
k_{pAA}, k_{pBB}	homopropagation rate constants in the polymer phase (dm^3/mol min.)
k_{pAB}, k_{pBA}	cross-propagation rate constants in the polymer phase (dm^3/mol min.)
M	polymer molecular weight (g/mol)
M_A	53.06 g/mol = molecular weight of A
M_B	54.09 g/mol = molecular weight of B
M_{eff}	effective molecular weight of an average repeating unit (g/mol)
m_i	mass of reagent i (i = A, B, copolymer, water, and initiator) (Kg)
$\bar{M}_n$, $\bar{B}_w$	number- and weight-average molecular weights (g/mol)
$[M]_p$	total monomer concentration in the polymer phase (mol/dm^3)
M_X	202.4 g/mol = molecular weight of X
N_{Av}	Avogadro's constant (1/mol)
N_i	moles of reagent i (i = A, B, X) (mol)
N_p	total number of polymer particles (dimensionless)
$\bar{n}$	average number of free radical per particle (dimensionless)
$\bar{p}_A$	average mass fraction of polymerized A in the copolymer (dimensionless)
p_{ref}	refrigerant pressure (atm)
Q_i	i-th (i = 0, 1, 2) moment of the number-chain length distribution (mol/dm^3)
Q_r	reaction heat rate (KJ/min.)
r_A, r_B	reactivity ratios of A and B (dimensionless)
R_{pA}, R_{pB}	consumption rates of monomers A, B (mol/min.)
t	time (min.)
T_a	ambient temperature (C)

T_i	inlet temperature of reagent i (i = A, X) (C)
T_r	reaction temperature (C)
T_{ref}	refrigerant temperature (C)
$V^0_{H_2O}$	initial volume of water (dm^3)
V_m, V_p	volumes of monomer phase and polymer phase (dm^3)
W_s	stirring power (KJ/min.)
x_g	gravimetric conversion (dimensionless)
X	chain transfer agent
y_A	average molar fraction of polymerized A in the accumulated copolymer (dimensionless)
Y_0	total moles of free radicals in the polymer phase (moles)

Greek Symbols

α	global heat transfer coefficient for the heat lost into the environment (J/K min.)
β	stirring heat coefficient (dimensionless)
γ	constant defined by Eq. A.12 (dimensionless)
ε	empirical exponent relating g and g' (dimensionless)
φ_A	fraction of A-terminated radical (dimensionless)
λ	"effective" latent heat of vaporization of the refrigerant (a propane–propylene mixture) (J/g)
Δt	time interval between two consecutive measurements (min.)
ΔH_A, ΔH_B	molar polymerization enthalpies of A, B (J/mol)

Superscripts

^{0}	indicates initial load or initial value
^{d}	indicates desired value (or set point)

APPENDIX A. ESTIMATION AND CONTROL ALGORITHMS

Molecular Weight Model

The kinetic scheme assumes that the following reactions take place in the polymer phase: propagation, termination, transfer to the comonomers, transfer to the chain transfer agent (CTA), transfer to the polymer (producing trifunctional branches), and propagation with the internal double bonds of the accumulated polymer (producing tetrafunctional branches). The main reagents are in equilibrium between phases with constant partition coefficients;[25] cross-propagation enthalpies are assumed identical to homopropagation enthalpies;[26,27] and the aqueous phase polymerization is neglected.[3]

With regards to molecular weights, the reaction is considered a homopolymerization, with the monomer concentration in the polymer particles equal

to $[M]_p = [A]_p + [B]_p$. Under semibatch conditions, the following mass balances may be written for the unreacted moles of CTA, N_X; the first three moments of the number chain-length distribution, Q_i (i=0,1,2); and the tri- and tetrafunctional branching frequencies, $\overline{B}_{N3}$ and $\overline{B}_{N4}$:[28]

$$\frac{dN_X}{dt} = \frac{F_{m,X}}{M_X} - k_p C_X [X]_p Y_0 \tag{A.1}$$

$$\frac{d(V_p Q_0)}{dt} = k_p [C_m [M]_p + C_X [X]_p - C_k Q_1] Y_0 \tag{A.2}$$

$$\frac{d(V_p Q_1)}{dt} = k_p [M]_p Y_0 \tag{A.3}$$

$$\frac{d(V_p Q_2)}{dt} = 2kp([M]_p + C_k Q_2) \frac{[M]_p + C_X [X]_p + (C_k + C_p) Q_2}{C_m [M]_p + C_X [X]_p + C_p Q_1} Y_0 \tag{A.4}$$

$$\frac{d(V_p Q_0 \overline{B}_{N3})}{dt} = k_p C_p Q_1 Y_0 \tag{A.5}$$

$$\frac{d(V_p Q_0 \overline{B}_{N4})}{dt} = k_p C_k Q_1 Y_0 \tag{A.6}$$

where $F_{m,X}$ is the mass flow rate of CTA; M_X is the CTA molecular weight; $[X]_p$ is the CTA concentration in the polymer particles; k_p is the pseudo rate constant of propagation; and C_X, C_m, C_p, and C_k, are ratios of pseudo rate constants (see Nomenclature). The total moles of free-radicals in the polymer phase are given by $Y_0 = \overline{n} N_P / N_{Av}$; where $\overline{n}$ is the average number of free radicals per particle, N_p is the total number of polymer particles, and N_{Av} is the Avogadro's constant.

The average molecular weights are calculated from:

$$\overline{M}_n = M_{eff} Q_1 / Q_0 \tag{A.7.a}$$

$$\overline{M}_w = M_{eff} Q_2 / Q_1 \tag{A.7.b}$$

where $M_{eff} = y_A M_A + (1 - y_A) M_B$ is the effective molecular weight of an hypothetical average repeating unit; y_A is the molar fraction of polymerized

A in the accumulated copolymer; and M_A, M_B are the molecular weights of A, B.

Heat Rate of Polymerization

At the discrete time k ($= t/\Delta t$), the instantaneously generated reaction heat, $Q_r(k)$, is calculated through the following discrete energy balance, which is an extension to the semibatch case of that presented in Gugliotta et al.:[16]

$$Q_r(k) = \left(C_p^{if} + \sum_j C_p^j\right)\frac{T_r(k) - T_r(k-1)}{\Delta t} - \sum_i F_{m,i}(k)c_p^i(T_i(k) - T_r(k)) + \lambda F_{m,ref}(k) + \alpha(T_r(k) - T_a(k)) - \beta W_s(k) \quad \text{(A.8)}$$

where C_p^{if} is the heat capacity of the internal fittings; c_p^i is the specific heat of reagent i (i = A, X); C_p^j ($= m_j c_p^j$) is the heat capacity of component j; m_j is the mass of component j (j = A, B, X, water, copolymer); λ is the "effective" latent heat of vaporization of the propane–propylene refrigerant; and α, β are constants that have been previously evaluated in Gugliotta et al.[16] On the r.-h.-s. of Eq. A.8, the first term represents the heat accumulated in the reaction mass and internal fittings (e.g., baffles and stirrer); the second term is the heat flow introduced by the feed of A or X; the third term is the heat flow removed by the refrigerant; the fourth term is the heat flow lost into the environment through the insulator; and the last term is the heat flow introduced by the stirrer.

Estimation of the Number–Average Number of Branches per Molecule

Estimates of the tri- and tetrafunctional number of branches per molecule, $\overline{B}_{N3}(k)$ and $\overline{B}_{N4}(k)$, are obtained from the discrete versions of Eqs. A.5 and A.6, yielding:

$$V_p(k+1)Q_0(k+1)\overline{B}_{N3}(k+1) = V_p(k)Q_0(k)\overline{B}_{N3}(k) + \Delta t k_p C_p Q_1(k) Y_0(k) \quad \text{(A.9.a)}$$

$$V_p(k+1)Q_0(k+1)\overline{B}_{N4}(k+1) = V_p(k)Q_0(k)\overline{B}_{N4}(k) + \Delta t k_p C_k Q_1(k) Y_0(k) \quad \text{(A.9.b)}$$

In Eqs. A.9.a,b, $V_p(k)$, $Q_0(k)$, and $Q_1(k)$ are all estimated from $Q_r(k)$;[16] while $Y_0(k)$ is calculated following Gugliotta et al.:[27]

$$Y_0(k) = \left(\frac{r_A[A]_p(k)}{k_{pAA}} + \frac{r_B[B]_p(k)}{k_{pBB}}\right)\left[\left(r_A[A]_p^2(k) + [A]_p(k)[B]_p(k)\right)\times(-\Delta H_A) + \left(r_B[B]_p^2(k) + [A]_p(k)[B]_p(k)\right)\times(-\Delta H_B)\right]^{-1} Q_r(k) \quad \text{(A.10)}$$

where k_{pAA}, k_{pBB} are the homopropagation rate constants of A, B; r_A, r_B are the reactivity ratios of A, B; and ΔH_A, ΔH_B are the molar polymerization enthalpies of A, B. In Eq. A.10, note that Y_0 is directly obtained from Q_r, without requiring a particle nucleation model.

Copolymer Composition Control via Semibatch Addition of A

An optimal (minimum-time) addition policy is proposed. It consists of initially charging the reactor with all of the less-reactive monomer (B) plus the amount of the more reactive monomer (A) that is required for producing (at the reaction start) the desired mass composition $\overline{p}_A^d$. Then, the remaining A is added to ensure that $\overline{p}_A(k) = \overline{p}_A^d$. The required mass profile of A, $F_{m,A}$, is calculated from Ref. 3:

$$F_{m,A}(k+1) = M_A\frac{N_A(k) - N_A(k-1)}{\Delta t} + M_A\frac{k_{pAA}k_{pBB}\gamma(1+\gamma r_A)}{k_{pBB}r_A\gamma + k_{pAA}r_B}\times[B]_p(k)Y_0(k) \quad \text{(A.11)}$$

where N_A are the moles of unreacted A, and γ is a constant obtained from:

$$\gamma = \frac{[A]_p^0}{[B]_p^0} = \frac{[A]_p(k)}{[B]_p(k)} = \frac{K - 1 + \left[(K-1)^2 + 4r_A r_B K\right]^{0.5}}{2r_A} \quad \text{(A.12)}$$

with

$$K = \frac{M_B\overline{p}_A^d}{M_A(1 - \overline{p}_A^d)} \quad \text{(A.13)}$$

where $[A]_p^0$, $[B]_p^0$ are the comonomer concentrations in the polymer particles at the initial time; and K is a constant.

An expression for the required initial moles of A may be derived from the algebraic equations that evaluate the phase volumes and the comonomer concentrations in the polymer and aqueous phases, yielding:

$$\begin{aligned} N_A^0 = {} & \gamma K_{Awp}\{\gamma K_{Amp}K_{Amw}M_A N_B^0\rho_B + K_{Bmp}\rho_A\rho_B V_{H_2O}^0 \\ & - K_{Amw}[\gamma K_{Awp}M_A N_B^0\rho_B + K_{Bwp}\rho_A(M_B N_B^0 - K_{Bmw}M_B N_B^0 \\ & + \rho_B V_{H_2O}^0)]\}/\{K_{Bmp}[(K_{Bmp} - K_{Bwp})M_B\rho_A \\ & + \gamma(K_{Amp} - K_{Awp})M_A\rho_B]\} \end{aligned} \tag{A.14}$$

where K_{imw}, K_{iwp}, and K_{imp} ($= K_{imw}K_{iwp}$), respectively, represent the partition coefficients of monomer i (i = A, B) between the following phases: monomer and aqueous, aqueous and polymer, and monomer and polymer; ρ_A, ρ_B are the densities of A, B; N_B^0 are the initial moles of B; and $V_{H_2O}^0$ is the initial water volume.

In the limit of the pseudo-bulk condition for the partitioning of A and B (i.e., when $[A]_p/[B]_p = N_A/N_B$, where N_B are the unreacted moles of B), the required feed profile of A is proportional to the instantaneously generated heat of reaction.[29] Thus,

$$F_{m,A}(k) = \frac{M_A(K-\gamma)}{(-\Delta H_B) + K(-\Delta H_A)}Q_r(k) \tag{A.15}$$

Control of Molecular Weights and Degrees of Branching via Addition of CTA

Initially, the reactor must be loaded with the needed amount of CTA for initially producing the desired value of $\overline{M}_w$ or $\overline{B}_{N3}$. Then, the required CTA mass flow rate, $F_{m,X}$, is obtained from the discrete version of Eq. A.1, i.e.,:

$$F_{m,X}(k+1) = M_X\left[\frac{N_X(k) - N_X(k-1)}{\Delta t} + k_p C_X[X]_p^d(k)Y_0(k)\right] \tag{A.16}$$

where $[X]_p^d$ is the required concentration of CTA in the polymer particles. In the following, consider the way of obtaining $[X]_p^d$ in each of the investigated control strategies.

a) $\overline{M}_w$ Control. To maintain a uniform $\overline{M}_w(k) = \overline{M}_w^d$, the required CTA concentration is obtained from (Eqs. A.3, A.4, and A.7.b), yielding:

$$[X]_p^d(k) = [M]_p\frac{\overline{M}_w^d\left(C_m + \frac{C_pQ_1}{[M]_p}\right) - 2M_{eff}\left(1 + \frac{C_kQ_2}{[M]_p}\right)\left(1 + \frac{(C_p + C_k)Q_2}{[M]_p}\right)}{C_X\left[2M_{eff}\left(1 + \frac{C_kQ_2}{[M]_p}\right) - \overline{M}_w^d\right]} \tag{A.17}$$

b) $\overline{B}_{N3}$ Control. Consider the production of a copolymer with any prespecified profile $\overline{B}_{N3}(k) = \overline{B}_{N3}^d(k)$. The required CTA concentration $[X]_p^d(k)$ is calculated as follows. First, the desired profile of $Q_0(k)$ is obtained from the discrete version of Eq. A.5, yielding:

$$Q_0^d(k) = \frac{k_pC_p\Delta t\sum_{j=1}^{k}Q_1(j)Y_0(j)}{V_p(k)B_{N3}^d(k)} \tag{A.18}$$

Then, the desired CTA concentration is obtained from Eqs. A.2 and A.5, that finally provide:

$$\begin{aligned} [X]_p^d(k) = {} & \frac{C_pQ_1(k)}{C_X\overline{B}_{N3}^d(k)} + \frac{V_p(k)Q_0^d(k)}{C_Xk_pY_0(k)\Delta t}\left(\frac{\overline{B}_{N3}^d(k)}{\overline{B}_{N3}^d(k-1)} - 1\right) \\ & - \frac{C_m[M]_p(k)}{C_X} + \frac{C_kQ_1(k)}{C_X} \end{aligned} \tag{A.19}$$

In both control policies, the initial amount of X, N_X^0, is obtained by solving a set of algebraic equations for: i) the CTA concentration in the polymer particles, ii) the ratio of CTA to monomer in the polymer particles required for producing the desired $\overline{M}_w$ or $\overline{B}_{N3}$, iii) the comonomer concentrations in the polymer and aqueous phases, and iv) the volumes of the monomer and aqueous phases. The procedure is similar to that described in Gugliotta et al.,[30] for the $\overline{M}_n$ control of an emulsion homopolymerization.

Virtual P+D Controller for the Molecular Weights and Branching

Eq. A.16 may lead to numerical errors as a consequence of a potential amplification of the measurement noise in the discrete algorithm. In particular,

these errors were observed during the $\overline{B}_{N3}$ control. To overcome this problem, the $\overline{B}_{N3}$ profile can be alternatively calculated applying a classical proportional-derivative (P+D) controller, as follows:

$$F_{m,X}(k+1) = K_p e(k) + T_D[e(k) - e(k-1)] \quad \text{(A.20.a)}$$

$$e(k) = y(k) - y^d(k) \quad \text{(A.20.b)}$$

where y^d is the desired value of either $\overline{M}_w$ or $\overline{B}_{N3}$; $e(k)$ is the error in the controlled variable at the discrete time k; and K_p, T_D are the controller parameters.

Despite the noisy measurements, the P+D controller proved adequate for calculating the required CTA flow. This is because most of the noise was filtered-off by the slow process dynamics. An integral action was not included to favor a fast system response.

ACKNOWLEDGMENTS

We are grateful to Pecom Energía S.A. for providing us with the experimental data and with the polymer samples. We also thank CONICET, SeTCIP, and Universidad Nacional del Litoral for the financial support.

REFERENCES

1. Kirk, R.E.; Othmer, D.F. *Encyclopedia of Chemical Technology*, 3rd Ed.; New York, 1981; Vol. 1, 427–442.
2. Ambler, M.R. Studies on the nature of multiple glass tansitions in low acrylonitrile, butadiene-acrylonitrile rubbers. J. Polym. Sci., Polym. Chem. Ed. **1973**, *11*, 1505–1515.
3. Vega, J.R.; Gugliotta, L.M.; Bielsa, R.O.; Brandolini, M.C.; Meira, G.R. Emulsion copolymerization of acrylonitrile and butadiene. Mathematical model of an industrial reactor. Ind. Eng. Chem. Res. **1997**, *36*, 1238–1246.
4. Dubé, M.A.; Penlidis, A.; Mutha, R.K.; Cluett, W.R. Mathematical modeling of emulsion copolymerization of acrylonitrile/butadiene. Ind. Eng. Chem. Res. **1996**, *35*, 4434–4448.
5. Rodríguez, V.I.; Estenoz, D.A.; Gugliotta, L.M.; Meira, G.R. Emulsion copolymerization of acrylonitrile and butadiene. Calculation of the detailed macromolecular structure. Int. J. Polym. Mater. **2001**, *in press*.
6. Leiza, J.R.; de la Cal, J.C.; Meira, G.R. Asua, J.M. On-line copolymer composition control in the semi-continuous emulsion copolymerization of ethyl acrylate and methyl methacrylate. Polym. React. Eng. **1993**, *1* (4), 461–498.
7. Canegallo, S.; Canu, P.; Morbidelli, M.; Storti, G. Composition control in emulsion copolymerization. II. Application to binary and ternary systems. J. Appl. Polym. Sci. **1994**, *54*, 1919.
8. Van den Brink, M.; Pepers, M.; van Herk, A.M.; German, A.L. On-line monitoring and control of the emulsion copolymerization of veova and butyl acrylate by raman spectroscopy. Polym. React. Eng. **2001**, *9* (2), 101–133.
9. Sáenz de Buruaga, I.; Arotçarena, M.; Armitage, P.D.; Gugliotta, L.M.; Leiza, J.R.; Asua, J.M. On-line calorimetric control of emulsion polymerization reactors. Chem. Eng. Sci. **1996**, *51*, 2781–2786.
10. Sáenz de Buruaga, I.; Echevarría, A.; Armitage, P.D.; de la Cal, J.C.; Leiza, J.R.; Asua, J.M. On-line control of a semi-batch emulsion polymerization reactor based on calorimetry. AIChE J. **1997**, *43*, 1069–1081.
11. Sáenz de Buruaga, I.; Armitage, P.D.; Leiza, J.R.; Asua, J.M. Nonlinear control for maximum production rate of latexes of well-defined polymer composition. Ind. Eng. Chem. Res. **1997**, *36*, 4243–4254.
12. Sáenz de Buruaga, I.; Armitage, P.D.; Leiza, J.R.; Asua, J.M. Model-based control of emulsion terpolymers based on calorimetric measurements. Polym. React. Eng. **2000**, *8* (1), 39–75.
13. Vicente, M.; BenAmor, S.; Gugliotta, L.M.; Leiza, J.R.; Asua, J.M. Control of molecular weight distribution in emulsion polymerization using on-line reaction calorimetry. Ind. Eng. Chem. Res. **2001**, *40*, 218–227.
14. Vicente, M.; Leiza, J.R.; Asua, J.M. Simultaneous control of the copolymer composition and molecular weight distribution in emulsion copolymerization. Ind. Eng. Chem. Res. **2001**, *in press*.
15. Kozub, D.J.; MacGregor, J.F. Feedback control of polymer quality in semi-batch copolymerization reactors. Chem. Eng. Sci. **1992**, *47*, 929–942.
16. Gugliotta, L.M.; Vega, J.R.; Antonione, C.E.; Meira, G.R. Emulsion copolymerization of acrylonitrile and butadiene in an industrial batch reactor. Estimation of conversion and polymer quality from on-line energy measurements. Polym. React. Eng. **1999**, *7* (4), 531–552.
17. Kolthoff, I.M.; Sandell, E.B.; Meehan, E.J.; Bruckenstein, S. *Quantitative Chemical Analysis*, 4th Ed.; Macmillan: New York, 1969.
18. Zimm, B.; Stockmayer, W. The dimensions of chain molecules containing branches and rings. J. Chem. Phys. **1949**, *17*, 1301–1314.
19. Vega, J.R.; Estenoz, D.A.; Oliva, H.M.; Meira, G.R. Analysis of a styrene-

butadiene graft copolymer by size exclusion chromatography. II. Determination of the branching exponent with the help of a polymerization model. Int. J. Polym. Anal. Charact. **2001**, *6*, 339–348.
20. Graessley, W.W.; Mittelhauser, H.M. Intrinsic viscosity of polydisperse branched polymers. J. Polym. Sci., Part A-2 **1967**, *5*, 431–454.
21. Small, P. Long chain branching in polymers. Adv. Polym. Sci. **1975**, *18*, 1–64.
22. Choi, K.Y.; Butala, D.N. Synthesis of open-loop controls for semibatch copolymerization reactors by inverse feedback control method. Automatika **1989**, *25* (6), 917–923.
23. Brandrup, J.; Immergut, E.H. *Polymer Handbook*, 3rd Ed.; Wiley & Sons: New York, 1989.
24. Broadhead, T. Dynamic Modeling of the Emulsion Copolymerization of Styrene/Butadiene. M. Eng. Thesis; McMaster University: Hamilton, Ontario, Canada, 1984.
25. Gugliotta, L.M.; Arzamendi, G.; Asua, J.M. Choice of monomer partition model in mathematical modeling of emulsion copolymerization systems. J. Appl. Polym. Sci. **1995**, *55*, 1017–1039.
26. Urretabizkaia, A.; Sudol, E.D.; El-Aasser, M.S.; Asua, J.M. Calorimetric monitoring of emulsion copolymerization reactions. J. Polym. Sci., Polym. Chem. **1993**, *31*, 2907–2913.
27. Gugliotta, L.M.; Arotçarena, M.; Leiza, J.R.; Asua, J.M. Estimation of conversion and copolymer composition in semicontinuous emulsion polymerization using calorimetric data. Polymer **1995**, *36* (10), 2019–2023.
28. Gugliotta, L.M.; Brandolini, M.C.; Vega, J.R.; Iturralde, E.O.; Azum, J.M.; Meira, G.R. Dynamic model of a continuous emulsion copolymerization of styrene and butadiene. Polym. React. Eng. **1995**, *3* (3), 201–233.
29. Gugliotta, L.M.; Leiza, J.R.; Arotçarena, M.; Armitage, P.D.; Asua, J.M. Copolymer composition control in unseeded emulsion polymerization using calorimetric data. Ind. Eng. Chem. Res. **1995**, *34*, 3899–3906.
30. Gugliotta, L.M.; Salazar, A.; Vega, J.R.; Meira, G.R. Emulsion polymerization of styrene. Use of n-nonyl mercaptan for molecular weight control. Polymer **2001**, *42*, 2719–2726.

Received September 7, 2001
Accepted January 9, 2002

POLYMER REACTION ENGINEERING, 10(1&2), 83–99 (2002)

EFFECT OF REGRIND ON THE PROPERTIES OF EXTRUDED PE PIPES

Sh. V. Mamedov,* V. A. Alekperov,* and Y. Lenger Özcanli

Yildiz Technical University, Department of Physics, Davutpasa Cad. 34010, Topkapı, İstanbul, Turkey

ABSTRACT

In this paper, the mechanical and thermo-oxidative degradation properties of samples made from high-density polyethylene (HDPE) pipes containing "regrind" from 5% to 50% have been investigated and compared with the structure changes of these samples. The results of tensile strength tests under constant σ, long- and short-term internal pressure tests, heat processes measurements, the values of density, Melt Flow Index (MFI), and Oxygen Induction Time (OIT) of samples produced from virgin resins were compared with international standards. It has been observed that the addition of regrind to raw resin in ratios 20–30% gives good results (This is due to the molecular structure of semicrystalline polymer). Since the "regrind" material fills amorphous part, the ratio of amorphous to crystalline parts of the virgin resin determines the amount of the "regrind" to be added.

*Current address: Inst. of Physics of the Azerbaijan Academy of Scien., Bakü, H. Javid St. 33, Azerbaijan.